This article was downloaded by: *[Aguilar, Luis T.]*
On: *28 April 2009*
Access details: *Access Details: [subscription number 910769851]*
Publisher *Taylor & Francis*
Informa Ltd Registered in England and Wales Registered Number: 1072954 Registered office: Mortimer House, 37-41 Mortimer Street, London W1T 3JH, UK

International Journal of Control
Publication details, including instructions for authors and subscription information:
http://www.informaworld.com/smpp/title~content=t713393989

Generating self-excited oscillations for underactuated mechanical systems via two-relay controller

Luis T. Aguilar [a]; Igor Boiko [b]; Leonid Fridman [c]; Rafael Iriarte [c]
[a] Instituto Politécnico Nacional, Centro de Investigación y Desarrollo de Tecnología Digital, San Ysidro, CA, USA [b] University of Calgary, 2500 University Dr. NW, Calgary, Alberta, Canada [c] Engineering Faculty, Department of Control, Universidad Nacional Autónoma de México (UNAM), Mexico City, Mexico

First Published on: 23 April 2009

To cite this Article Aguilar, Luis T., Boiko, Igor, Fridman, Leonid and Iriarte, Rafael(2009)'Generating self-excited oscillations for underactuated mechanical systems via two-relay controller',International Journal of Control,

To link to this Article: DOI: 10.1080/00207170802657363

URL: http://dx.doi.org/10.1080/00207170802657363

PLEASE SCROLL DOWN FOR ARTICLE

Full terms and conditions of use: http://www.informaworld.com/terms-and-conditions-of-access.pdf

This article may be used for research, teaching and private study purposes. Any substantial or systematic reproduction, re-distribution, re-selling, loan or sub-licensing, systematic supply or distribution in any form to anyone is expressly forbidden.

The publisher does not give any warranty express or implied or make any representation that the contents will be complete or accurate or up to date. The accuracy of any instructions, formulae and drug doses should be independently verified with primary sources. The publisher shall not be liable for any loss, actions, claims, proceedings, demand or costs or damages whatsoever or howsoever caused arising directly or indirectly in connection with or arising out of the use of this material.

International Journal of Control
2009, 1–14, iFirst

Taylor & Francis
Taylor & Francis Group

Generating self-excited oscillations for underactuated mechanical systems via two-relay controller

Luis T. Aguilar[a]*, Igor Boiko[b], Leonid Fridman[c] and Rafael Iriarte[c]

[a]*Instituto Politécnico Nacional, Centro de Investigación y Desarrollo de Tecnología Digital, PMB 88, PO Box 439016, San Ysidro, CA, USA;* [b]*University of Calgary, 2500 University Dr. NW, Calgary, Alberta, Canada;* [c]*Engineering Faculty, Department of Control, Universidad Nacional Autónoma de México (UNAM), CP 04510, Mexico City, Mexico*

(*Received 1 April 2008; final version received 30 November 2008*)

A tool for the design of a periodic motion in an underactuated mechanical system via generating a self-excited oscillation of a desired amplitude and frequency by means of the variable structure control is proposed. First, an approximate approach based on the describing function method is given, which requires that the mechanical plant should be a linear low-pass filter – the hypothesis that usually holds when the oscillations are relatively fast. The method based on the locus of a perturbed relay systems provides an exact model of the oscillations when the plant is linear. Finally, the Poincaré map's design provides the value of the controller parameters ensuring the locally orbitally stable periodic motions for an arbitrary mechanical plant. The proposed approach is shown by the controller design and experiments on the Furuta pendulum.

Keywords: variable structure systems; underactuated systems; periodic solution; frequency domain methods

Downloaded By: [Aguilar, Luis T.] At: 20:24 28 April 2009

1. Introduction

1.1 *Overview*

In this article, we consider the control of one of the simplest types of a functional motion: generation of a periodic motion in underactuated mechanical systems which could be of non-minimum-phase. Current representative works on periodic motions in an orbital stabilisation of underactuated systems involve finding and using a reference model as a generator of limit cycles (e.g. Orlov, Riachy, Floquet, and Richard (2006)), thus considering the problem of obtaining a periodic motion as a servo problem. Orbital stabilisation of underactuated systems finds applications in the coordinated motion of biped robots (Chevallereau et al. 2003), gymnastic robots and others (see, e.g., Grizzle, Moog, and Chevallereau (2005), Shiriaev, Freidovich, Robertsson, and Sandberg (2007) and references therein).

1.2 *Methodology*

In this article, underactuated systems are considered as the systems with internal (unactuated) dynamics with respect to the actuated variables. It allows us to propose a method of generating a periodic motion in an underactuated system where the same behaviour can be seen via second-order sliding mode (SOSM) algorithms, i.e. generating self-excited oscillations using the same mechanism as the one that produces chattering. However, the generalisation of the SOSM algorithms and the treatment of the unactuated part of the plant as additional dynamics result in the oscillations that may not necessarily be fast and of small amplitude.

There exist two approaches to analysis of periodic motions in the sliding mode systems due to the presence of additional dynamics: the time-domain approach, which is based on the state-space representation, and the frequency-domain approach. The Poincaré maps (Varigonda and Georgiou 2001) are successfully used to ensure the existence and stability of periodic motions in the relay control systems (see Di Bernardo, Johansson, and Vasca (2001), Fridman (2001) and references therein). The describing function (DF) method (see, e.g., Atherton (1975)) offers finding approximate values of the frequency and the amplitude of periodic motions in the systems with linear plants driven by the sliding mode controllers. The locus of perturbed relay system (LPRS) method (Boiko 2005) provides an exact solution of the periodic problem in discontinuous control systems, including finding exact values of the amplitude and the frequency of the self-excited oscillation.

*Corresponding author. Email: luis.aguilar@ieee.org

ISSN 0020–7179 print/ISSN 1366–5820 online
© 2009 Taylor & Francis
DOI: 10.1080/00207170802657363
http://www.informaworld.com

Downloaded By: [Aguilar, Luis T.] At: 20:24 28 April 2009

1.3 *Results of this article*

The proposed approach is based on the fact that all SOSM algorithms (Boiko, Fridman, and Castellanos 2004; Boiko, Fridman, Pisano, and Usai 2007) produce chattering (periodic motions of relatively small amplitude and high frequency) in the presence of unmodelled dynamics. In sliding mode control, chattering is usually considered an undesirable component of the motion. In this article, we aim to use this property of SOSM for the purpose of generating a relatively slow motion with a significantly higher amplitude and lower frequency than respectively the amplitude and frequency of chattering.

The twisting algorithm (Levant 1993) originally created as a SOSM controller – to ensure the finite-time convergence – is generalised, so that it can generate self-excited oscillations in the closed-loop system containing an underactuated plant. The required frequencies and amplitudes of periodic motions are produced without tracking of precomputed trajectories. It allows for generating a wider (than the original twisting algorithm with additional dynamics) range of frequencies and encompassing a variety of plant dynamics.

A systematic approach is proposed to find the values of the controller parameters allowing one to obtain the desired frequencies and the output amplitude, which includes:

- an approximate approach based on the DF method that requires for the plant to be a low-pass filter;
- a design methodology based on LPRS that gives exact values of controller parameters for the linear plants;
- an algorithm that uses Poincaré maps and provides the values of the controller parameters ensuring the existence of the locally orbitally stable periodic motions for an arbitrary mechanical plant.

The theoretical results are validated experimentally via the tests on the laboratory Furuta pendulum. The periodic motion is generated around the upright position (which gives the non-minimum phase system case).

1.4 *Organisation of this article*

This article is structured as follows. Section 2 introduces the problem statement. In Section 3, the idea of the two-relay controller is explained via the frequency domain methods. In Section 4 the approximate values of controller parameters are computed via the DF method and stability of the periodic solution will be provided. In Section 5, the LPRS method is provided to compute the exact values of the controller parameters. In Section 6, the Poincaré method will be used as a design tool. An example is provided in Section 7 in order to illustrate the design methodologies given in Sections 4–6. In Section 8, the design methodology is validated via periodic motion design for the experimental Furuta pendulum. Section 9 provides final conclusions.

2. Problem statement

Let the underactuated mechanical system, which is a plant in the system where a periodic motion is supposed to occur, be given by the Lagrange equation:

$$M(q)\ddot{q} + H(q,\dot{q}) = B_1 u \tag{1}$$

where $q \in \mathbb{R}^m$ is the vector of joint positions; $u \in \mathbb{R}$ is the vector of applied joint torques where $m<n$; $B_1 = [0_{(m-1)}, 1]^T$ is the input that maps the torque input to the joint coordinates space; $M(q) \in \mathbb{R}^{m\times m}$ is the symmetric positive-definite inertia matrix; and $H(q,\dot{q}) \in \mathbb{R}^m$ is the vector that contains the Coriolis, centrifugal, gravity and friction torques. The following two-relay controller is proposed for the purpose of exciting a periodic motion:

$$u = -c_1 \operatorname{sign}(y) - c_2 \operatorname{sign}(\dot{y}), \tag{2}$$

where c_1 and c_2 are parameters designed such that the scalar output of the system (the position of a selected link of the plant)

$$y = h(q) \tag{3}$$

has a steady periodic motion with the desired frequency and amplitude.

Let us assume that the two-relay controller has two independent parameters $c_1 \in C_1 \subset \mathbb{R}$ and $c_2 \in C_2 \subset \mathbb{R}$, so that the changes to those parameters result in the respective changes of the frequency $\Omega \in \mathcal{W} \subset \mathbb{R}$ and the amplitude $A_1 \in \mathcal{A} \subset \mathbb{R}$ of the self-excited oscillations. Then we can note that there exist two mappings $F_1 : C_1 \times C_2 \mapsto \mathcal{W}$ and $F_2 : C_1 \times C_2 \mapsto \mathcal{A}$, which can be rewritten as $F : C_1 \times C_2 \mapsto \mathcal{W} \times \mathcal{A} \subset \mathbb{R}^2$. Assume that mapping F is unique. Then there exists an inverse mapping $G : \mathcal{W} \times \mathcal{A} \mapsto C_1 \times C_2$. The objective is, therefore, (a) to obtain mapping G using a frequency-domain method for deriving the model of the periodic process in the system, (b) to prove the uniqueness of mappings F and G for the selected controller and (c) to find the ranges of variation of Ω and A_1 that can be achieved by varying parameters c_1 and c_2.

The *analysis and design objectives* are formulated as follows: find the parameter values c_1 and c_2 in (2) such that the system (1) has a periodic motion with the desired frequency Ω and desired amplitude of the

output signal A_1. Therefore, the main objective of this research is to find mapping G to be able to tune c_1 and c_2 values.

3. The idea of the method

The idea of the method is to provide the mapping from a set of desired frequencies $\mathcal{W} \subset \mathbb{R}$ and amplitudes $\mathcal{A} \subset \mathbb{R}$ into a set of gain values $\mathcal{C} \subset \mathbb{R}^2$, that is $G : \mathcal{W} \times \mathcal{A} \mapsto \mathcal{C}$. To achieve the objective, let us start with the design via the DF method which is a useful frequency-domain tool for time-invariant linear plants to predict the existence or absence of limit cycles and estimate the frequency and amplitude when it exists. In the scenario introduced in Boiko et al. (2004), the DF method was used for analysis of chattering for the closed-loop system with the twisting algorithm where the inverse of this mapping was derived.

3.1 *Some specific features of underactuated systems*

To begin with, let us consider the following underactuated system called cart-pendulum (Fantoni and Lozano 2001, p. 26):

$$\begin{bmatrix} M+m & ml\cos\theta \\ ml\cos\theta & ml^2 \end{bmatrix} \begin{bmatrix} \ddot{x} \\ \ddot{\theta} \end{bmatrix} + \begin{bmatrix} F_v\dot{\theta} - ml\sin\theta\dot{\theta}^2 \\ -mgl\sin\theta \end{bmatrix} = \begin{bmatrix} u \\ 0 \end{bmatrix} \tag{4}$$

where $x \in \mathbb{R}$ is the linear position of the cart along the horizontal axis, $\theta \in \mathbb{R}$ is the rotational angle of the pendulum, $M = 1.035\,\mathrm{kg}$ and $m = 0.165\,\mathrm{kg}$ are the masses of the cart and the inverted pendulum, respectively; $l = 0.2425\,\mathrm{m}$ is the distance from the centre of gravity of the link to its attachment point, $F_v = 1.0\,\mathrm{N\,m\,s\,rad^{-1}}$ is the viscous friction coefficient, and $g = 9.81\,\mathrm{m\,s^{-2}}$ is the gravitational acceleration constant (see Figure 1). Linearising around the unstable equilibrium point ($\theta = 0$) and substituting the value of the parameters, the transfer function from the angle of the pendulum θ to the input u is

$$W(s) = \frac{\Theta(s)}{U(s)} = \frac{1}{0.1s+1} \cdot \frac{1}{0.25\,(s^2+s-2887)}. \tag{5}$$

Note that the Nyquist plot of the above transfer function is located in the second quadrant of the complex plane.

4. DF of the two-relay controller

Let first, the linearised plant be given by:

$$\begin{aligned} \dot{x} &= Ax + Bu \\ y &= Cx \end{aligned}, \quad x \in \mathbb{R}^n, \quad y \in \mathbb{R}, \quad n = 2m \tag{6}$$

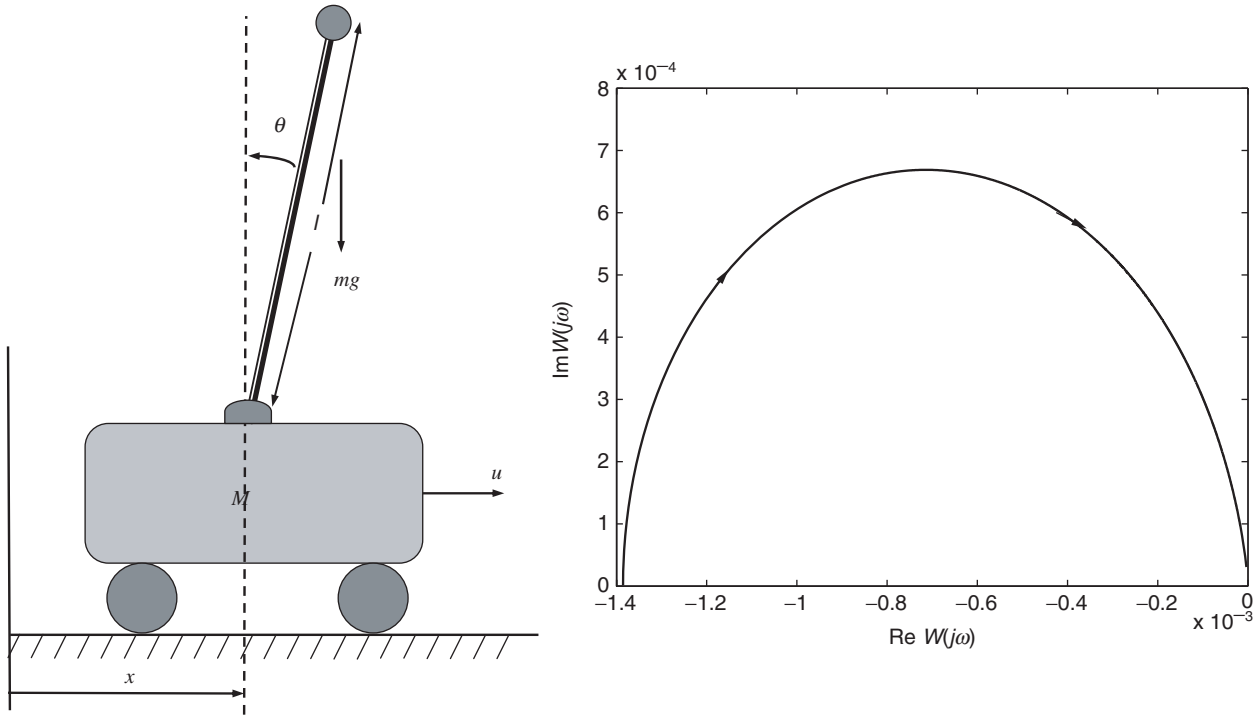

Figure 1. The cart-pendulum system and its corresponding Nyquist plot of transfer function from the angle of the pendulum to the input of the actuator.

Downloaded By: [Aguilar, Luis T.] At: 20:24 28 April 2009

Downloaded By: [Aguilar, Luis T.] At: 20:24 28 April 2009

which can be represented in the transfer function form as follows:

$$W(s) = C(sI - A)^{-1}B.$$

Let us assume that matrix A has no eigenvalues at the imaginary axis and the relative degree of (6) is greater than 1.

The DF, N, of the variable structure controller (2) is the first harmonic of the periodic control signal divided by the amplitude of $y(t)$ (Atherton 1975):

$$N = \frac{\omega}{\pi A_1}\int_0^{2\pi/\omega} u(t)\sin\omega t\,\mathrm{d}t + j\frac{\omega}{\pi A_1}\int_0^{2\pi/\omega} u(t)\cos\omega t\,\mathrm{d}t \tag{7}$$

where A_1 is the amplitude of the input to the non-linearity (of $y(t)$ in our case) and ω is the frequency of $y(t)$. However, the algorithm (2) can be analysed as the parallel connection of two ideal relays where the input to the first relay is the output variable and the input to the second relay is the derivative of the output variable (Figure 1). For the first relay the DF is:

$$N_1 = \frac{4c_1}{\pi A_1},$$

and for the second relay it is (Atherton 1975):

$$N_2 = \frac{4c_2}{\pi A_2},$$

where A_2 is the amplitude of $\mathrm{d}y/\mathrm{d}t$. Also, take into account the relationship between y and $\mathrm{d}y/\mathrm{d}t$ in the Laplace domain, which gives the relationship between the amplitudes A_1 and A_2: $A_2 = A_1\Omega$, where Ω is the frequency of the oscillation. Using the notation of the algorithm (2) we can rewrite this equation as follows:

$$N = N_1 + sN_2 = \frac{4c_1}{\pi A_1} + j\Omega\frac{4c_2}{\pi A_2} = \frac{4}{\pi A_1}(c_1 + jc_2), \tag{8}$$

where $s = j\Omega$. Let us note that the DF of the algorithm (2) depends on the amplitude value only. This suggests the technique of finding the parameters of the limit cycle – via the solution of the harmonic balance equation (Atherton 1975):

$$W(j\Omega)N(a) = -1, \tag{9}$$

where a is the generic amplitude of the oscillation at the input to the non-linearity, and $W(j\omega)$ is the complex frequency response characteristic (Nyquist plot) of the plant. Using the notation of the algorithm (2) and replacing the generic amplitude with the amplitude of the oscillation of the input to the first relay this equation can be rewritten as follows:

$$W(j\Omega) = -\frac{1}{N(A_1)}, \tag{10}$$

where the function at the right-hand side is given by:

$$-\frac{1}{N(A_1)} = \pi A_1\frac{-c_1 + jc_2}{4(c_1^2 + c_2^2)}.$$

Equation (9) is equivalent to the condition of the complex frequency response characteristic of the open-loop system intersecting the real axis in the point $(-1, j0)$. The graphical illustration of the technique of solving (9) is given in Figure 2. The function $-1/N$ is a straight line the slope of which depends on c_2/c_1 ratio. The point of intersection of this function and of the Nyquist plot $W(j\omega)$ provides the solution of the periodic problem (Figure 3).

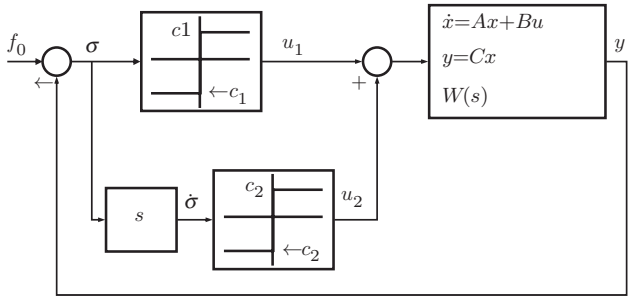

Figure 2. Relay feedback system.

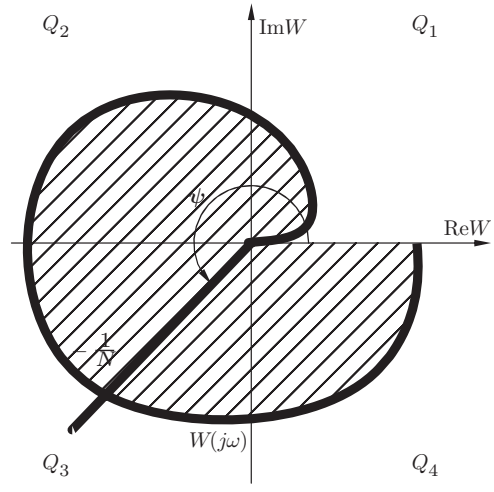

Figure 3. Example of a Nyquist plot of the open-loop system $W(j\omega)$ with two-relay controller.

Downloaded By: [Aguilar, Luis T.] At: 20:24 28 April 2009

4.1 *Tuning the parameters of the controller*

Here, we summarise the steps to tune c_1 and c_2:

(a) Identify the quadrant in the Nyquist plot where the desired frequency Ω is located, which falls into one of the following categories (sets):

$$Q_1 = \{\omega \in \mathbb{R} : \mathrm{Re}\{W(j\omega)\} > 0, \mathrm{Im}\{W(j\omega)\} \geq 0\}$$
$$Q_2 = \{\omega \in \mathbb{R} : \mathrm{Re}\{W(j\omega)\} \leq 0, \mathrm{Im}\{W(j\omega)\} \geq 0\}$$
$$Q_3 = \{\omega \in \mathbb{R} : \mathrm{Re}\{W(j\omega)\} \leq 0, \mathrm{Im}\{W(j\omega)\} < 0\}$$
$$Q_4 = \{\omega \in \mathbb{R} : \mathrm{Re}\{W(j\omega)\} > 0, \mathrm{Im}\{W(j\omega)\} < 0\}.$$

(b) The frequency of the oscillations depends only on the c_2/c_1 ratio, and it is possible to obtain the desired frequency Ω by tuning the $\xi = c_2/c_1$ ratio:

$$\xi = \frac{c_2}{c_1} = -\frac{\mathrm{Im}\{W(j\Omega)\}}{\mathrm{Re}\{W(j\Omega)\}}. \tag{11}$$

Since the amplitude of the oscillations is given by

$$A_1 = \frac{4}{\pi}|W(j\Omega)|\sqrt{c_1^2 + c_2^2}, \tag{12}$$

then the c_1 and c_2 values can be computed as follows:

$$c_1 = \begin{cases} \dfrac{\pi}{4} \cdot \dfrac{A_1}{|W(j\Omega)|} \cdot \left(\sqrt{1+\xi^2}\right)^{-1} & \text{if } \Omega \in Q_2 \cup Q_3 \\ -\dfrac{\pi}{4} \cdot \dfrac{A_1}{|W(j\Omega)|} \cdot \left(\sqrt{1+\xi^2}\right)^{-1} & \text{elsewhere} \end{cases} \tag{13}$$

$$c_2 = \xi \cdot c_1. \tag{14}$$

4.2 *Stability of periodic solutions*

We shall consider that the harmonic balance condition still holds for small perturbations of the amplitude and the frequency with respect of the periodic motion. In this case the oscillation can be described as a damped one. If the damping parameter will be negative at a positive increment of the amplitude and positive at a negative increment of the amplitude then the perturbation will vanish, and the limit cycle will be asymptotically stable.

Theorem 1: *Suppose that for the values of the* c_1 *and* c_2 *given by* (13) *and* (14) *there exists a corresponding periodic solution to the systems* (2) *and* (6). *If*

$$\mathrm{Re}\frac{\mathrm{d}\arg W}{\mathrm{d}\ln\omega}\bigg|_{\omega=\Omega} \leq -\frac{c_1 c_2}{c_1^2 + c_2^2} \tag{15}$$

then the above-mentioned periodic solutions to the systems (2) *and* (6) *is orbitally asymptotically stable.*

Proof: The proof of this theorem is given in Aguilar, Boiko, Fridman, and Iriarte (2009). □

5. Locus of a perturbed relay system design

The LPRS proposed in Boiko (2005) provides an exact solution of the periodic problem in a relay feedback system having a plant (6) and the control given by the hysteretic relay. The LPRS is defined as a characteristic of the response of a linear part to an unequally spaced pulse control of variable frequency in a closed-loop system (Boiko 2005). This method requires a computational effort but will provide an exact solution. The LPRS can be computed as follows:

$$J(\omega) = \sum_{k=1}^{\infty}(-1)^{k+1}\mathrm{Re}\{W(k\omega)\} + j\sum_{k=1}^{\infty}\frac{1}{2k-1}\mathrm{Im}\big\{W[(2k-1)\omega]\big\}. \tag{16}$$

The frequency of the periodic motion for the algorithm (2) can be found from the following equation (Boiko 2005) (Figure 4):

$$\mathrm{Im}\, J(\Omega) = 0$$

In effect, we are going to consider the plant being non-linear, with the second relay transposed to the feedback in this equivalent plant. Introduction of the following function will be instrumental in finding a response of the non-linear plant to the periodic square-wave pulse control.

$$L(\omega,\theta) = \sum_{k=1}^{\infty}\frac{1}{2k-1}(\sin[(2k-1)2\pi\theta]\mathrm{Re}\{W[(2k-1)\omega]\} + \cos[(2k-1)2\pi\theta]\mathrm{Im}\{W[(2k-1)\omega]\}). \tag{17}$$

The function $L(\omega,\theta)$ denotes a linear plant output (with a coefficient) at the instant $t = \theta T$ (with T being

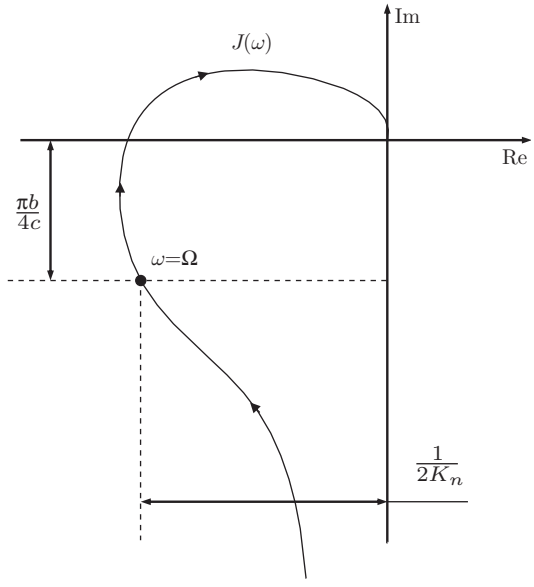

Figure 4. LPRS and oscillation analysis.

the period: $T=2\pi/\omega$) if a periodic square-wave pulse signal of amplitude $\pi/4$ is applied to the plant:

$$L(\omega,\theta)=\left.\frac{\pi y(t)}{4c}\right|_{t=2\pi\theta/\omega}$$

with $\theta\in[-0.5,0.5]$ and $\omega\in[0,\infty]$, where $t=0$ corresponds to the control switch from -1 to $+1$.

With $L(\omega,\theta)$ available, we obtain the following expression for $\mathrm{Im}\{J(\omega)\}$ of the equivalent plant:

$$\mathrm{Im}\{J(\omega)\}=L(\Omega,0)+\frac{c_2}{c_1}L(\Omega,\theta). \tag{18}$$

The value of the time shift θ between the switching of the first and second relay can be found from the following equation:

$$\dot{y}(\theta)=0.$$

As a result, the set of equations for finding the frequency Ω and the time shift θ is as follows:

$$\begin{aligned} c_1L(\Omega,0)+c_2L(\Omega,\theta)&=0\\ c_1L_1(\Omega,-\theta)+c_2L_1(\Omega,0)&=0. \end{aligned} \tag{19}$$

The amplitude of the oscillations can be found as follows. The output of the system is:

$$\begin{aligned} y(t)=\frac{4}{\pi}\sum_{i=1}^{\infty}\big\{&c_1\sin[(2k-1)\Omega+\varphi_L((2k-1)\Omega)]\\ &+c_2\sin[(2k-1)\Omega t+\varphi_L((2k-1)\Omega)\\ &+(2k-1)2\pi\theta]\big\}A_L((2k-1)\Omega) \end{aligned} \tag{20}$$

where $\varphi_L(\omega)=\arg W(\omega)$, which is a response of the plant to the two square pulse-wave signals shifted with respect to each other by the angle $2\pi\theta$. Therefore, the amplitude is

$$A_1=\max_{t\in[0;2\pi/\omega]}y(t). \tag{21}$$

Yet, instead of the true amplitude we can use the amplitude of the fundamental frequency component (first harmonic) as a relatively precise estimate. In this case, we can represent the input as the sum of two rotating vectors having amplitudes $4c_1/\pi$ and $4c_2/\pi$, with the angle between the vectors $2\pi\theta$. Therefore, the amplitude of the control signal (first harmonic) is

$$A_u=\frac{4}{\pi}\sqrt{c_1^2+c_2^2+2c_1c_2\cos(2\pi\theta)}, \tag{22}$$

and the amplitude of the output (first harmonic) is

$$A_1=\frac{4}{\pi}\sqrt{c_1^2+c_2^2+2c_1c_2\cos(2\pi\theta)}A_L(\Omega), \tag{23}$$

where $A_L(\omega)=|W(j\omega)|$. We should note that despite using approximate value for the amplitude in (23), the value of the frequency is exact.

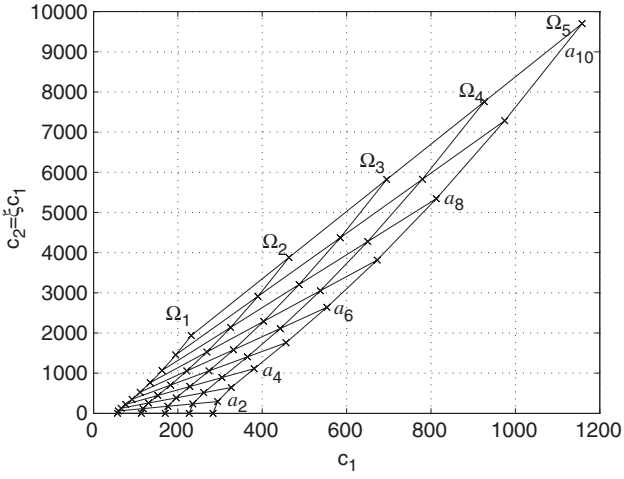

Figure 5. Plot of c_1 vs c_2 for arbitrary frequencies $\Omega_1<\Omega<\Omega_5$ and amplitudes $a_1<A_1<a_{10}$.

Expressions (19) and (23) if considered as equations for Ω and A_1 provide one with mapping F. This mapping is depicted in Figure 5 as curves of equal values of Ω and A_1 in the coordinates (c_1,c_2). From (19) one can see that the frequency of the oscillations depends only on the ratio $c_2/c_1=\xi$. Therefore, Ω is invariant with respect to c_2/c_1: $\Omega(\lambda c_1,\lambda c_2)=\Omega(c_1,c_2)$. It also follows from (23) that there is the following invariance for the amplitude: $A_1(\lambda c_1,\lambda c_2)=\lambda A_1(c_1,c_2)$. Therefore, Ω and A_1 can be manipulated independently in accordance with mapping G considered below.

Mapping G (inverse of F) can be derived from (19) and (23) if c_1, c_2 and θ are considered unknown parameters in those equations. For any given Ω, from Equation (19) the ratio $c_2/c_1=\xi$ can be found (as well as θ). Therefore, we can find first $\xi=c_2/c_1=h(\Omega)$, where $h(\Omega)$ is an implicit function that corresponds to (19). After that c_1 and c_2 can be computed as per the following formulas:

$$c_1=\frac{\pi}{4}\frac{A_1}{A_L(\Omega)}\frac{1}{\sqrt{1+2\xi\cos(2\pi\theta)+\xi^2}} \tag{24}$$

$$c_2=\frac{\pi}{4}\frac{A_1}{A_L(\Omega)}\frac{\xi}{\sqrt{1+2\xi\cos(2\pi\theta)+\xi^2}}. \tag{25}$$

6. Poincaré design

Poincaré map is a recognised tool for analysis of the existence of limit cycles for non-linear systems. Therefore, this tool is appropriate to satisfy the goal defined in Section 2. To begin with, let us consider that the actuated degrees of freedom are represented by the elements of $\eta=(\eta_1,\eta_2)\in\mathbb{R}^2$ and the unactuated

Downloaded By: [Aguilar, Luis T.] At: 20:24 28 April 2009

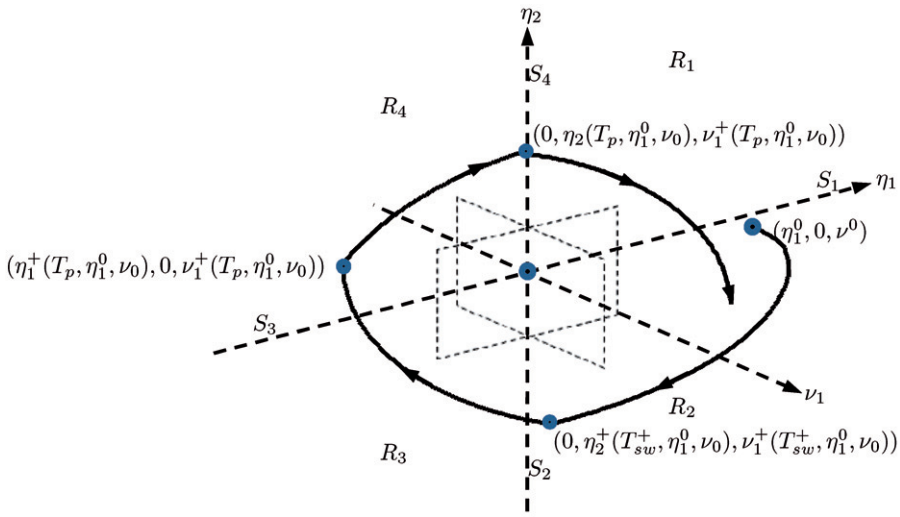

Figure 6. Partitioning of the state space and the Poincaré map.

Downloaded By: [Aguilar, Luis T.] At: 20:24 28 April 2009

degrees of freedom are represented by the elements of $\nu = (\nu_1, \nu_2) \in \mathbb{R}^{2m-2}$. Let us define the output $y = \eta_1$ The Lagrange equation (1) can be represented in the state-space form by:

$$\begin{bmatrix} \dot{\eta}_1 \\ \dot{\eta}_2 \\ \dot{\nu}_1 \\ \dot{\nu}_2 \end{bmatrix} = \begin{bmatrix} \eta_2 \\ \left\{ \begin{matrix} \Delta_m^{-1}\{M_{22}(\eta_1, \nu_1)[u - N_1(\eta, \nu)] \\ +M_{12}(\eta_1, \nu_1)N_2(\eta, \nu)\} \end{matrix} \right\} \\ \nu_2 \\ \left\{ \begin{matrix} \Delta_m^{-1}\{-M_{12}(\eta_1, \nu_1)[u - N_1(\eta, \nu)] \\ -M_{11}(\eta_1, \nu_1)N_2(\eta, \nu)\} \end{matrix} \right\} \end{bmatrix} = \begin{bmatrix} \eta_2 \\ f_1(\eta, \nu, u) \\ \nu_2 \\ f_2(\eta, \nu, u) \end{bmatrix} \tag{26}$$

where u is given in (2), and $\Delta_m = M_{11}(\eta_1, \nu_1) \times M_{22}(\eta_1, \nu_1) - M_{12}(\eta_1, \nu_1)M_{12}(\eta_1, \nu_1)$. Control law (2) switches on the surface $\eta_1 = 0$ and $\eta_2 = 0$. Consider the sets (Figure 6):

$$\begin{aligned} S_1 &= \{(\eta_1, \eta_2, \nu_1, \nu_2) : \eta_1 > 0, \eta_2 = 0\} \\ S_2 &= \{(\eta_1, \eta_2, \nu_1, \nu_2) : \eta_1 = 0, \eta_2 < 0\} \\ S_3 &= \{(\eta_1, \eta_2, \nu_1, \nu_2) : \eta_1 < 0, \eta_2 = 0\} \\ S_4 &= \{(\eta_1, \eta_2, \nu_1, \nu_2) : \eta_1 = 0, \eta_2 > 0\}. \end{aligned} \tag{27}$$

The space $\mathbb{R}^n$ is divided by S_i, into four regions $i = 1, \ldots, 4$, namely

$$\begin{aligned} R_1 &= \{(\eta_1, \eta_2, \nu_1, \nu_2) : \eta_1 > 0, \eta_2 > 0\}, \\ R_2 &= \{(\eta_1, \eta_2, \nu_1, \nu_2) : \eta_1 > 0, \eta_2 < 0\}, \\ R_3 &= \{(\eta_1, \eta_2, \nu_1, \nu_2) : \eta_1 < 0, \eta_2 < 0\}, \\ R_4 &= \{(\eta_1, \eta_2, \nu_1, \nu_2) : \eta_1 < 0, \eta_2 > 0\}. \end{aligned} \tag{28}$$

with $f_1 < 0$ for all $\eta_1, \eta_2, \nu \in R_1 \cup R_2$; and $f_1 > 0$ for all $\eta_1, \eta_2, \nu \in R_3 \cup R_4$. Assume that f_1 and f_2 are differentiable in the set R_i, $i = 1, \ldots, 4$. Moreover, suppose that the values of the functions of $f_k, k = 1, 2$ in the sets R_i could be smoothly extended till their closures $\bar{R}_i$. Considering (η_1, η_2), let us derive the Poincaré map from $\varphi_1(\cdot) = (\eta_1, 0)$, where $\eta_1 > 0$, into $\varphi_2(\cdot) = (0, \eta_2)$, where $\eta_2 < 0$ (see region R_2 in Figure 6). Let $\eta_1^0 > 0$ and denote as

$$\begin{matrix} \eta_1^+(t, \eta_1^0, \nu^0, c_1, c_2), & \eta_2^+(t, \eta_1^0, \nu^0, c_1, c_2) \\ \nu_1^+(t, \eta_1^0, \nu^0, c_1, c_2), & \nu_2^+(t, \eta_1^0, \nu^0, c_1, c_2) \end{matrix} \tag{29}$$

the solution of the system (26) with the initial conditions

$$\begin{aligned} &\eta_1^+(0, \eta_1^0, \nu^0, c_1, c_2) = \eta_1^0, \quad \eta_2^+(0, \eta_1^0, \nu^0, c_1, c_2) = 0, \\ &\nu^+(0, \eta_1, \nu^0, c_1, c_2) = \nu^0. \end{aligned} \tag{30}$$

Let $T_{sw}(\eta, \nu, c_1, c_2)$ be the smallest positive root of the equation

$$\eta_1^+(T_{sw}, \eta_1^0, \nu^0, c_1, c_2) = 0 \tag{31}$$

and such that $(\mathrm{d}\eta_1^+/\mathrm{d}t)(T_{sw}, \eta_1^0, \nu^0, c_1, c_2) = \eta_2^+(T_{sw}, \eta_1^0, \nu^0, c_1, c_2) < 0$, i.e. the functions

$$\begin{matrix} T_{sw}(\eta_1^0, \nu^0, c_1, c_2), & \eta_1^+(T_{sw}, \eta_1^0, \nu^0, c_1, c_2), \\ \eta_2^+(T_{sw}, \eta_1^0, \nu^0, c_1, c_2), & \nu^+(T_{sw}, \eta_1^0, \nu^0, c_1, c_2), \end{matrix}$$

smoothly depend on their arguments.

Now, let us derive the Poincaré map from the sets $\varphi_2(\cdot) = (0, \eta_2, \nu_1^0)$, where $\eta_2 < 0$, into the sets $\varphi_3(\cdot) = (\eta_1, 0, \nu_1^0)$ where $\eta_1 < 0$ (see region R_3 in Figure 6). To this end, denote as

$$\eta_{1p}^+(t, \eta_1^0, \nu^0, c_1, c_2), \quad \eta_{2p}^+(t, \eta_1^0, \nu^0, c_1, c_2), \quad \nu_p^+(t, \eta_1^0, \nu^0, c_1, c_2), \tag{32}$$

the solution of the system (26) with the initial conditions

$$\begin{aligned}
&\eta_{1p}^{+}(T_{sw}^{+}(\eta_1^0,\nu^0,c_1,c_2),\eta^0,\nu^0,c_1,c_2)=0,\\
&\eta_{2p}^{+}(T_{sw}^{+}(\eta_1^0,\nu^0,c_1,c_2),\eta^0,\nu^0,c_1,c_2)\\
&\quad=\eta_2^{+}(T_{sw}^{+}(\eta_1^0,\nu^0,c_1,c_2),\eta_1^0,\nu^0,c_1,c_2),\\
&\nu_p^{+}(T_{sw}^{+}(\eta_1^0,\nu^0,c_1,c_2),\eta^0,\nu^0,c_1,c_2)\\
&\quad=\nu_1^{+}(T_{sw}^{+}(\eta_1^0,\nu^0,c_1,c_2),\eta_1^0,\nu^0,c_1,c_2),
\end{aligned}\tag{33}$$

Let $T_p^+(\eta,\nu,c_1,c_2)$ be the smallest root satisfying the restrictions $T_p^+ > T_{sw}^+ > 0$ of the equation

$$\eta_{2p}^{+}(T_p^+,\eta_1^0,\nu^0,c_1,c_2)=0 \tag{34}$$

and such that $(\mathrm{d}\eta_2^+/\mathrm{d}t)(T_p^+)=f_1(T_p^+,\eta_1,\eta_2,\nu,c_1,c_2)<0$, i.e. the functions

$$\begin{aligned}
&T_p(\eta_1^0,\nu^0,c_1,c_2),\quad \eta_1^+(T_p,\eta_1^0,\nu^0,c_1,c_2),\\
&\eta_2^+(T_p,\eta_1^0,\nu^0,c_1,c_2),\quad \nu_1^+(T_p,\eta_1^0,\nu^0,c_1,c_2),\\
&\nu_2^+(T_p,\eta_1^0,\nu^0,c_1,c_2)
\end{aligned}$$

smoothly depend on their arguments. Therefore, we have designed the map

$$\Xi^{+}(\eta_1^0,\nu^0,c_1,c_2)=\begin{bmatrix}\eta_1^{+}(T_p^{+}(\eta_1^0,\nu^0,c_1,c_2),\eta_1^0,\nu^0,c_1,c_2)\\ \nu^{+}(T_p^{+}(\eta_1^0,\nu^0,c_1,c_2),\eta_1^0,\nu^0,c_1,c_2)\end{bmatrix} \tag{35}$$

The map $\Xi^-(\eta_1^0,\nu^0,c_1,c_2)$ of $\varphi_3(\cdot)=(\eta_1,0,\nu^0)$, $\eta_1<0$ starting at the point $\Xi^+(\eta_1^0,\nu^0,c_1,c_2)$ into $\varphi_1(\cdot)=(\eta_1,0)$, $\eta_1>0$ together with the time constant $T_p^+ < T_{sw}^- < T_p^-$ can be defined by the similar procedure.

Therefore the desired periodic solution corresponds to the fixed point of the Poincaré map (Figure 7)

$$\begin{bmatrix}\eta_1^\star\\ \nu^\star\end{bmatrix}-\Xi^{-}(T_p^-,\eta_1^\star,\nu^\star,c_1,c_2)=0. \tag{36}$$

Finally, to complete the design of periodic solution with desired period $T_p^- = 2\pi/\Omega$ and amplitude $\eta_1^\star = A_1$ the set of algebraic equations needs to be solved with respect to c_1, c_2, and ν^0:

$$\begin{aligned}
&\begin{bmatrix}A_1\\ \nu^\star\end{bmatrix}-\Xi^{-}(2\pi/\Omega,A_1,\nu^\star,c_1,c_2)=0,\\
&\qquad\eta_{2p}^{-}(2\pi/\Omega,A_1,\nu^\star,c_1,c_2)=0,
\end{aligned}\tag{37}$$

where c_1 and c_2, are unknown parameters.

Theorem 2: *Suppose that for the given value of amplitude A_1 and value of frequency Ω there exist c_1 and c_2 such the Poincaré map $\Xi(\eta_1^0,\nu^0,c_1,c_2)$ has a fixed point $[\eta_1^\star,\nu^\star]$ such that $T_p^-=2\pi/\Omega$, $\eta_1^\star = A_1$,*

$$\left\|\frac{\partial\Xi^{-}(\eta_1,\nu,c_1,c_2)}{\partial(\eta_1,\nu)}_{(A_1,\nu^\star)}\right\|<1 \tag{38}$$

holds. Then, the system (26) *has an orbitally asymptotically stable limit cycle with a desired period $2\pi/\Omega$ and amplitude A_1.*

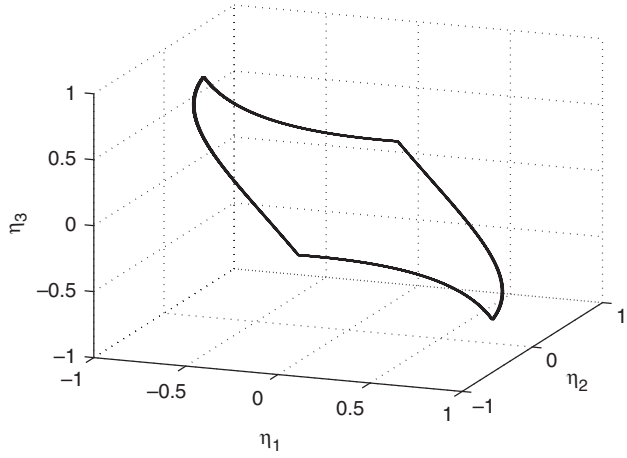

Figure 7. Evolution of the states η, ν of the closed-loop system.

7. Illustrative example

Let us consider the transfer function

$$W(s)=\frac{1}{(Js+1)(s^2+F_v s-a^2)},\quad J>0 \tag{39}$$

and its corresponding linear state-space representation

$$\begin{aligned}
&\frac{\mathrm{d}\eta_1}{\mathrm{d}t}=\eta_2\\
&\frac{\mathrm{d}\eta_2}{\mathrm{d}t}=\nu\\
&\frac{\mathrm{d}\nu}{\mathrm{d}t}=J^{-1}\left[a^2\eta_1-(F_v-Ja^2)\eta_2-(1+JF_v)\nu+u\right]
\end{aligned}\tag{40}$$

where $J=4/3$, $F_v=1/4$, $a=1/\sqrt{8}$, and

$$u=-c_1\,\mathrm{sign}(\eta_1)-c_2\,\mathrm{sign}(\eta_2) \tag{41}$$

is the two-relay controller which forces the output $y=\eta_1$ to have a periodic motion. In the example, we set $\Omega=1\,\mathrm{rad\,s^{-1}}$ and $A_1=0.7$.

Downloaded By: [Aguilar, Luis T.] At: 20:24 28 April 2009

Downloaded By: [Aguilar, Luis T.] At: 20:24 28 April 2009

7.1 *DF and LPRS*

First, we compute the value of c_1 and c_2 through DF by using the set of equations:

$$c_1 = \begin{cases} \frac{\pi}{4} \cdot \frac{A_1}{|W(j\Omega)|} \cdot \left(\sqrt{1+\xi^2}\right)^{-1} & \text{if } \Omega \in Q_2 \cup Q_3 \\ -\frac{\pi}{4} \cdot \frac{A_1}{|W(j\Omega)|} \cdot \left(\sqrt{1+\xi^2}\right)^{-1} & \text{elsewhere} \end{cases}$$

$$c_2 = \xi \cdot c_1.$$

where $\xi = c_2/c_1$, obtaining $c_1 = 0.8018$ and $c_2 = 0.78$.

To check if the periodic solution is stable find the derivative of the phase characteristic of the plant with respect to the frequency

$$\left.\frac{d\arg W}{d\ln\omega}\right|_{\omega=\Omega} = -\left.\frac{d\arctan(J\omega)}{d\ln\omega}\right|_{\omega=\Omega} + \left.\frac{d\arctan(\frac{F_v\omega}{\omega^2+a^2})}{d\ln\omega}\right|_{\omega=\Omega}$$

$$= -\frac{J\Omega}{J^2\Omega^2+1} + \frac{F_v\Omega(a^2-\Omega^2)}{F_v^2\Omega^2+(a^2+\Omega^2)^2}. \quad (42)$$

The stability condition (15) for the system becomes:

$$-\frac{J\Omega}{J^2\Omega^2+1} + \frac{F_v\Omega(a^2-\Omega^2)}{F_v^2\Omega^2+(a^2+\Omega^2)^2} \le -\frac{\xi}{\xi^2+1}. \quad (43)$$

Notice that the left-hand side of (40) is -0.6447 and the right-hand side is -0.4998. Therefore, the system is orbitally asymptotically stable.

Now, let us compute the exact values of c_1 and c_2 through LPRS by using the following formulas:

$$c_1 = \frac{\pi}{4}\frac{A_1}{A_L(\Omega)}\frac{1}{\sqrt{1+2\xi\cos(2\pi\theta)+\xi^2}},$$

$$c_2 = \frac{\pi}{4}\frac{A_1}{A_L(\Omega)}\frac{\xi}{\sqrt{1+2\xi\cos(2\pi\theta)+\xi^2}},$$

obtaining $c_1 = 0.7017$ and $c_2 = 0.6015$, with simulation results given in Figure 8.

7.2 *Poincaré map design*

Let us begin with the mapping from φ_1 into the set φ_2 (region R_2) where the system (40) takes the form:

$$\frac{d\eta_1}{dt} = \eta_2, \quad \frac{d\eta_2}{dt} = \nu, \quad \frac{d\nu}{dt} = \frac{3}{32}\eta_1 - \frac{1}{16}\eta_2 - \nu - \frac{3}{4}c_1 + \frac{3}{4}c_2. \quad (44)$$

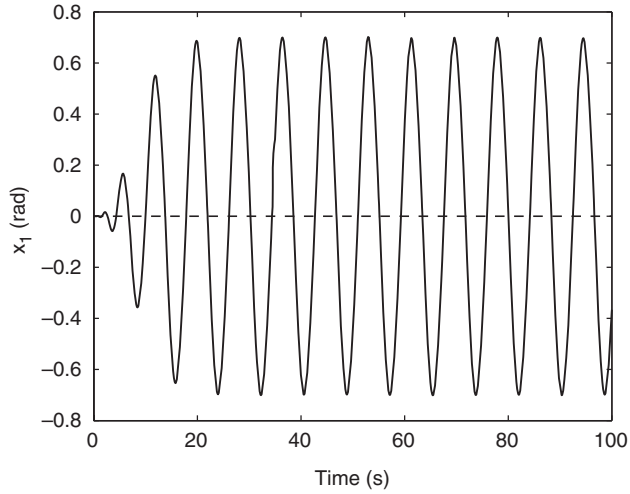

Figure 8. Simulation results for the systems (2) and (40) under c_1 and c_2 computed through LPRS method.

The solution of (44) on the time interval $[0, T_{sw}]$ subject to the initial condition:

$$\eta_1^+(\eta_1^0, \nu^0, c_1, c_2) = \eta_1^0 > 0, \quad \eta_2^+(\eta_1^0, \nu^0, c_1, c_2) = 0,$$
$$\nu^+(\eta_1^0, \nu^0, c_1, c_2) = \nu_1^0$$

results in

$$\eta_1^+ = \underbrace{8c_1 - 8c_2}_{\gamma_1} + \underbrace{\left(8c_2 - 8c_1 + \eta_1^0 - \frac{16}{3}\nu_1^0\right)}_{\gamma_2(\eta_1^0,\nu^0,c_1,c_2)} e^{-t/2}$$
$$+ \underbrace{\left(4c_2 - 4c_1 + \frac{1}{2}\eta_1^0 + \frac{4}{3}\nu_1^0\right)}_{\gamma_3(\eta_1^0,\nu^0,c_1,c_2)} e^{t/4} \quad (45)$$
$$+ \underbrace{\left(4c_1 - 4c_2 - \frac{1}{2}\eta_1^0 + 4\nu_1^0\right)}_{\gamma_4(\eta_1^0,\nu^0,c_1,c_2)} e^{-3t/4} \quad (46)$$

$$\eta_2^+ = -\frac{1}{2}\gamma_2(\eta_1^0, \nu^0, c_1, c_2)e^{-t/2} + \frac{1}{4}\gamma_3(\eta_1^0, \nu^0, c_1, c_2)e^{t/4}$$
$$- \frac{3}{4}\gamma_4(\eta_1^0, \nu^0, c_1, c_2)e^{-3t/4} \quad (47)$$

$$\nu^+ = \frac{1}{4}\gamma_2(\eta_1^0, \nu^0, c_1, c_2)e^{-t/2} + \frac{1}{16}\gamma_3(\eta_1^0, \nu^0, c_1, c_2)e^{t/4}$$
$$+ \frac{9}{16}\gamma_4(\eta_1^0, \nu^0, c_1, c_2)e^{-3t/4}, \quad (48)$$

where

$$T_{sw}(\eta_1^0, \nu^0, c_1, c_2) = 4\ln z, \quad z = e^{t/4} \quad (49)$$

is obtained as the smallest positive root of

$$\eta_1^+(T_{sw},\eta_1^0,\nu^0,c_1,c_2)=\gamma_3 z^4+\gamma_1 z^3+\gamma_2 z+\gamma_4=0, \tag{50}$$

where $\gamma_1=\gamma_1(\eta_1^0,\nu^0,c_1,c_2)$, $\gamma_2=\gamma_2(\eta_1^0,\nu^0,c_1,c_2)$, and $\gamma_3=\gamma_3(\eta_1^0,\nu^0,c_1,c_2)$. Let us proceed with the mapping from φ_2 into φ_3 (region R_3) where the system (39) takes the form:

$$\frac{\mathrm{d}\eta_1}{\mathrm{d}t}=\eta_2,\quad \frac{\mathrm{d}\eta_2}{\mathrm{d}t}=\nu,\quad \frac{\mathrm{d}\nu}{\mathrm{d}t}=\frac{3}{32}\eta_1-\frac{1}{16}\eta_2-\nu+\frac{3}{4}c_1+\frac{3}{4}c_2. \tag{51}$$

The solution of (51) on the time interval $[T_{sw},T_p]$ subject to the initial condition:

$$\eta_{1sw}^+=\eta_{1p}^+(T_{sw},\eta_1^0,c_1,c_2)=0,$$
$$\eta_{2sw}^+=\eta_{2p}^+(T_{sw},\eta_1^0,c_1,c_2)=-\frac{1}{2}\gamma_2 e^{-T_{sw}/2}+\frac{1}{4}\gamma_3 e^{T_{sw}/4}-\frac{3}{4}\gamma_4 e^{-3T_{sw}/4}$$

results in

$$\eta_{1p}^+=-8c_1-8c_2+8\underbrace{\left(c_1+c_2-\frac{1}{3}\eta_{2sw}^+\right)}_{\gamma_{1p}(\eta_1^0,\nu^0,c_1,c_2)}e^{-(t-T_{sw})/2}-4\underbrace{\left(c_1+c_2-\frac{1}{4}\eta_{2sw}^+\right)}_{\gamma_{2p}(\eta_1^0,\nu^0,c_1,c_2)}e^{-3(t-T_{sw})/4}+4\underbrace{\left(c_1+c_2+\frac{5}{12}\eta_{2sw}^+\right)}_{\gamma_{3p}(\eta_1^0,\nu^0,c_1,c_2)}e^{(t-T_{sw})/4} \tag{52}$$

$$\eta_{2p}^+=-4\gamma_{1p}e^{-(t-T_{sw})/2}+3\gamma_{2p}e^{-3(t-T_{sw})/4}+\gamma_{3p}e^{(t-T_{sw})/4} \tag{53}$$

$$\eta_{3p}^+=2\gamma_{1p}e^{-(t-T_{sw})/2}-\frac{9}{4}\gamma_{2p}e^{-3(t-T_{sw})/4}+\frac{1}{4}\gamma_{3p}e^{(t-T_{sw})/4} \tag{54}$$

where $\gamma_{1p}=\gamma_{1p}(\eta_1^0,\nu^0,c_1,c_2)$, $\gamma_{2p}=\gamma_{2p}(\eta_1^0,\nu^0,c_1,c_2)$, $\gamma_{3p}=\gamma_{3p}(\eta_1^0,\nu^0,c_1,c_2)$ and

$$T_p(\eta_1^0,\nu^0,c_1,c_2)=4\ln z_p+T_{sw},\quad z_p=e^{(t-T_{sw})/4} \tag{55}$$

results from the the smallest positive root of

$$\eta_{2p}^+(T_p,\eta_1^0,\nu^0,c_1,c_2)=\gamma_{3p}z_p^4-4\gamma_{1p}z_p+3\gamma_{2p}=0. \tag{56}$$

Then, the Poincaré map is

$$\Xi_1^+(T_p(\eta_1^0,\nu^0,c_1,c_2),\eta_1^0,\nu^0,c_1,c_2)=\begin{bmatrix}\gamma_1+\gamma_2e^{-T_p/2}+\gamma_3e^{T_p/4}+\gamma_4e^{-3T_p/4}\\ \frac{1}{4}\gamma_2e^{-T_p/2}+\frac{1}{16}\gamma_3e^{T_p/4}+\frac{9}{16}\gamma_4e^{-3T_p/4}\end{bmatrix} \tag{57}$$

and the fixed point that is the solution of

$$-\begin{bmatrix}\eta_1^0\\ \nu^0\end{bmatrix}=\Xi_1^+(T_p(\eta_1^0,\nu^0,c_1,c_2),\eta^0,\nu^0,c_1,c_2)$$

which results in

$$(\eta_1^0)^\star=-\frac{\left\{\begin{array}{l}\gamma_1+[8c_2-8c_1-\frac{16}{3}\nu_1^0]e^{-T_p/2}+[4c_2-4c_1\\ \quad+\frac{4}{3}\nu_1^0]e^{T_p/4}+[4c_1-4c_2+4\nu_1^0]e^{-3T_p/4}\end{array}\right\}}{1+e^{-\Delta T/2}+\frac{1}{2}e^{\Delta T/4}-\frac{1}{2}e^{-3\Delta T/4}}$$

$$(\nu_1^0)^\star=\frac{\left\{\begin{array}{l}\frac{1}{4}[8c_2-8c_1+\eta_1^0]e^{-T_p/2}+\frac{1}{16}[4c_2-4c_1\\ \quad+\frac{1}{2}\eta_1^0]e^{T_p/4}+\frac{9}{16}[4c_1-4c_2+\frac{1}{2}\eta_1^0]e^{-3T_p/4}\end{array}\right\}}{\frac{4}{3}e^{-T_p/2}-\frac{1}{12}e^{T_p/4}-\frac{9}{4}e^{-3T_p/4}}$$

where $\Delta T=T_p-T_{sw}$. To complete the design it remains to provide the set of equations to find c_1 and c_2 in terms of the known parameters T_p and η_1^0. Towards this end, we obtain from above equations that c_1 and c_2 are solution of the following set of equations:

$$c_2-c_1=\frac{1}{4}\cdot\frac{\left\{\begin{array}{l}-[1+e^{-T_p/2}+\frac{1}{2}e^{T_p/4}-\frac{1}{4}e^{-3T_p/4}](\eta_1^0)^\star\\ \quad-\gamma_1+(\frac{16}{3}e^{-T_p/2}-\frac{4}{3}e^{T_p/4}-4e^{-3T_p/4})\nu_1^0\end{array}\right\}}{2e^{-T_p/2}+e^{T_p/4}-e^{-3T_p/4}} \tag{58}$$

$$c_2+c_1=\frac{\left\{\begin{array}{l}\left[\frac{4}{3}e^{-T_p/2}-\frac{1}{12}e^{T_p/4}-\frac{9}{4}e^{-3T_p/4}\right](\nu^0)^\star\\ \quad-\left[\frac{1}{4}e^{-T_p/2}+\frac{1}{32}e^{T_p/4}+\frac{9}{32}e^{-3T_p/4}\right]\eta_1^0\end{array}\right\}}{2e^{-T_p/2}+\frac{1}{4}e^{T_p/4}-\frac{9}{4}e^{-3T_p/4}}. \tag{59}$$

Then, for a given frequency $T_1+T_2=2\pi/\Omega$ and amplitude $\eta_1^0=A_1$ we obtain that $c_1=0.7017$ and $c_2=0.6027$. Finally, we need to check the stability, i.e.

$$\left\|\left.\frac{\partial\Xi_1^+((\eta_1^0)^\star,(\nu^0)^\star,c_1,c_2)}{\partial(\eta_1^0,\nu^0)}\right|_{(\eta_1^0)^\star,(\nu^0)^\star}\right\|=\left\|\begin{bmatrix}\left.\frac{\partial\Xi_{11}^+((\eta_1^0)^\star,(\nu^0)^\star,c_1,c_2)}{\partial\eta_1^0}\right|_{(\eta_1^0)^\star,(\nu^0)^\star} & \left.\frac{\partial\Xi_{11}^+((\eta_1^0)^\star,(\nu^0)^\star,c_1,c_2)}{\partial\nu^0}\right|_{(\eta_1^0)^\star,(\nu^0)^\star}\\ \left.\frac{\partial\Xi_{21}^+((\eta_1^0)^\star,(\nu^0)^\star,c_1,c_2)}{\partial\eta_1^0}\right|_{(\eta_1^0)^\star,(\nu^0)^\star} & \left.\frac{\partial\Xi_{21}^+((\eta_1^0)^\star,(\nu^0)^\star,c_1,c_2)}{\partial\nu^0}\right|_{(\eta_1^0)^\star,(\nu^0)^\star}\end{bmatrix}\right\|<1, \tag{60}$$

Downloaded By: [Aguilar, Luis T.] At: 20:24 28 April 2009

Downloaded By: [Aguilar, Luis T.] At: 20:24 28 April 2009

where

$$\frac{\partial \Xi_{11}^{+}(\eta_1^0, \nu^0, c_1, c_2)}{\partial \eta_1^0} = -\left[-\frac{1}{2}\gamma_2 e^{-T_p/2} + \frac{1}{4}\gamma_3 e^{T_p/4} - \frac{3}{4}\gamma_4 e^{-3T_p/4}\right]\frac{\partial T_p}{\partial \eta_1^0} + e^{-T_p/2} + \frac{1}{2}e^{T_p/4} - \frac{1}{2}e^{-3T_p/4} \simeq -0.4416 \quad (61)$$

$$\frac{\partial \Xi_{11}^{+}(\eta_1^0, \nu^0, c_1, c_2)}{\partial \nu^0} = -\left[-\frac{1}{2}\gamma_2 e^{-T_p/2} + \frac{1}{4}\gamma_3 e^{T_p/4} - \frac{3}{4}\gamma_4 e^{-3T_p/4}\right]\frac{\partial T_p}{\partial \nu^0} - \frac{16}{3}e^{-T_p/2} + \frac{3}{4}e^{T_p/4} + 4e^{-3T_p/4} \simeq 0.1745 \quad (62)$$

$$\frac{\partial \Xi_{21}^{+}(\eta_1^0, \nu^0, c_1, c_2)}{\partial \eta_1^0} = -\left[-\frac{1}{8}\gamma_2 e^{-T_p/2} + \frac{1}{64}\gamma_3 e^{T_p/4} - \frac{27}{64}\gamma_4 e^{-3T_p/4}\right]\frac{\partial T_p}{\partial \eta_1^0} + \frac{1}{4}e^{-T_p/2} + \frac{1}{16}e^{T_p/4} + \frac{9}{16}e^{-3T_p/4} \simeq 0.2088 \quad (63)$$

$$\frac{\partial \Xi_{21}^{+}(\eta_1^0, \nu^0, c_1, c_2)}{\partial \nu^0} = -\left[-\frac{1}{8}\gamma_2 e^{-T_p/2} + \frac{1}{64}\gamma_3 e^{T_p/4} - \frac{27}{64}\gamma_4 e^{-3T_p/4}\right]\frac{\partial T_p}{\partial \nu^0} - \frac{4}{3}e^{-T_p/2} + \frac{1}{12}e^{T_p/4} + \frac{9}{4}e^{-3T_p/4} \simeq 0.1042, \quad (64)$$

$$\frac{\partial T_{sw}}{\partial \eta_1^0} = 4 \cdot \frac{\frac{1}{2}z^{-4} - z^{-3} + \frac{1}{2}z^{-1} + 1 - \frac{1}{2}z^{3}}{-4\gamma_3 z^3 - 3\gamma_1 z^2 - \gamma_2 + \gamma_3 - 2\gamma_2 z^{-3} - 3\gamma_4 z^{-4}} \simeq -0.6399,$$

$$\frac{\partial T_{sw}}{\partial \nu^0} = 4 \cdot \frac{4z^{-4} - \frac{16}{3}z^{-3} - 4z^{-1} + \frac{20}{3} - \frac{4}{3}z^{3}}{4\gamma_3 z^3 + 3\gamma_1 z^2 + \gamma_2 - \gamma_3 + 2\gamma_2 z^{-3} + 3\gamma_4 z^{-4}} \simeq 1.4989,$$

$$\frac{\partial T_p}{\partial \eta_1^0} = \frac{4}{z_p} \cdot \frac{\frac{\partial \eta_{2p}^{+}}{\partial \eta_1^0} - \left[\frac{5}{12}z_p^4 + \frac{4}{3}z_p - \frac{3}{4}\right]\frac{\partial \eta_{2sw}^{+}}{\partial \eta_1^0}}{4\gamma_{3p}z_p^3 - 4\gamma_{1p}} + \frac{\partial T_{sw}}{\partial \eta_1^0} \simeq -2.4002,$$

$$\frac{\partial T_p}{\partial \nu^0} = \frac{4}{z_p} \cdot \frac{\frac{\partial \eta_{2p}^{+}}{\partial \nu^0} - \left[\frac{5}{12}z_p^4 + \frac{4}{3}z_p - \frac{3}{4}\right]\frac{\partial \eta_{2sw}^{+}}{\partial \nu^0}}{4\gamma_{3p}z_p^3 - 4\gamma_{1p}} + \frac{\partial T_{sw}}{\partial \nu^0} \simeq -1.0468,$$

$\partial \eta_{2p}^{+}/\partial \eta_1^0 \simeq -9.8782$, and $\partial \eta_{2p}^{+}/\partial \nu^0 \simeq -1.5876$. Using (60), we have

$$\left\| \left. \frac{\partial \Xi_1^{+}(\eta_1^0, \nu^0, c_1, c_2)}{\partial (\eta_1^0, \nu^0)} \right|_{(\eta_1^0)^\star, (\nu^0)^\star} \right\| = \left\| \begin{bmatrix} -0.4416 & 0.1745 \\ 0.2088 & 0.1042 \end{bmatrix} \right\| \simeq 0.5030$$

where $\|\mathcal{A}\| = \sqrt{\lambda_{\max}\{\mathcal{A}^T\mathcal{A}\}}$; therefore, it is verified that the orbit is asymptotically stable.

8. Experimental study: the Furuta pendulum

8.1 *Experimental setup*

In this section, we present experimental results using the laboratory Furuta pendulum, produced by Quanser Consulting Inc., depicted in Figure 9. It consists of a 24 V DC motor that is coupled with an encoder and is mounted vertically in the metal chamber. The L-shaped arm, or hub, is connected to the motor shaft and pivots between ±180 degrees. At the end, a suspended pendulum is attached. The pendulum angle is measured by the encoder. As described in Figure 9, the arm rotates about z-axis and its angle is denoted by q_1 while the pendulum attached to the arm rotates about its pivot and its angle is called q_2. The experimental setup includes a PC equipped with an NI-M series data acquisition card connected to the Educational Laboratory Virtual Instrumentation Suite (NI-ELVIS) workstation from National Instrument. The controller was implemented using Labview programming language allowing debugging, virtual oscilloscope, automation functions, and data storage during the experiments. The sampling frequency for control implementation has been set to 400 Hz. Appendix A gives the dynamic model of the Furuta pendulum.

8.2 *Experimental results*

Experiments were carried out to achieve the orbital stabilisation of the unactuated link (the pendulum) $y = q_2$ around the equilibrium point $q^\star = (\pi, 0)$. The equation of motion of the Furuta pendulum (13) is linearised around $q^\star \in \mathbb{R}^2$ and by virtue of the instability of the linearised open-loop system, a state-feedback controller $u_f = -Kx$ and $x = (q - q^\star, \dot{q})^T \in \mathbb{R}^4$, is designed such that the compensated system has an overshoot of 8 and gain crossover frequency at 10 rad s^{-1} (see Bode diagram in Figure 10 for the open-loop system). Thus, the matrices A, B, and C of the linear

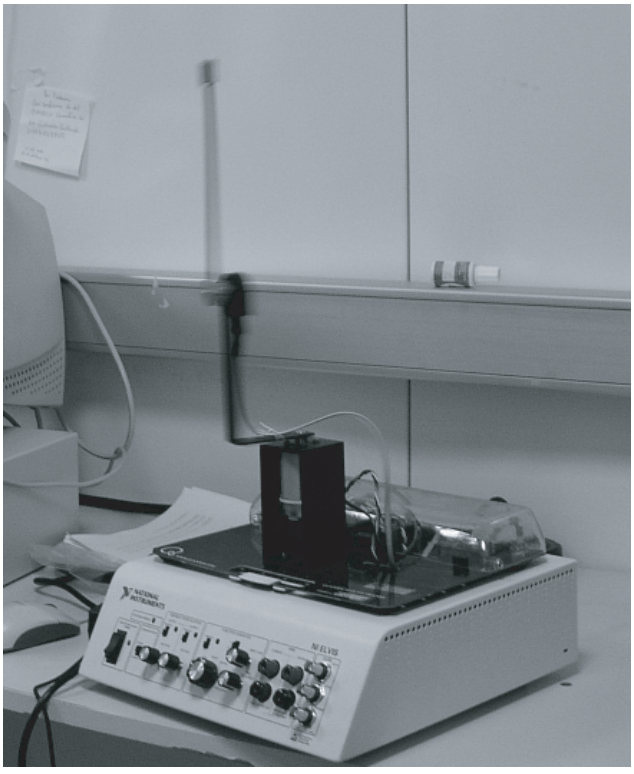

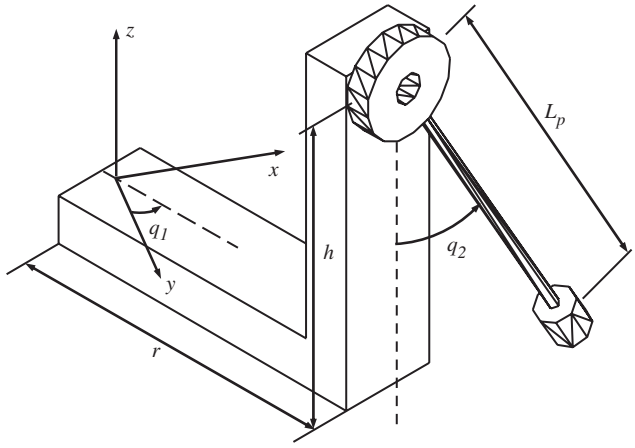

Figure 9. The experimental Furuta pendulum system.

system (6) are

$$A = \begin{bmatrix} 0 & 0 & 1 & 0 \\ 0 & 0 & 0 & 1 \\ -6.591 & 125.685 & -6.262 & 25.525 \\ 3.031 & -112.408 & 2.879 & -11.737 \end{bmatrix},$$

$$B = \begin{bmatrix} 0 \\ 0 \\ 56.389 \\ -25.930 \end{bmatrix}, \quad C = \begin{bmatrix} 0 \\ 1 \\ 0 \\ 0 \end{bmatrix}^T.$$

For the experiments, we set initial conditions sufficiently close to the equilibrium point $q^\star \in \mathbb{R}^2$. The output $y = q_2$ is driven to a periodic motion for several desired frequencies and amplitudes. The frequencies (Ω) and amplitudes (A_1) obtained from experiments by using the values of c_1 and c_2 computed by means of the DF and LPRS are given in Tables 1 and 2, respectively. Inequality (27) holds for the chosen frequencies and amplitudes, thus asymptotical stability of the periodic orbit was established by Theorem 1.

In Figure 11, experimental oscillations for the output y, for fast ($\Omega_1 = 25\,\mathrm{rad\,s^{-1}}$) and slow motion ($\Omega_2 = 10\,\mathrm{rad\,s^{-1}}$) are displayed. Note that certain imperfections appear in the slow motion graphics in Figure 11, which are attributed to the Coulomb friction forces and the dead zone. Also, in some modes natural frequencies of the pendulum mechanical structure are excited, and manifested as higher-frequency vibrations.

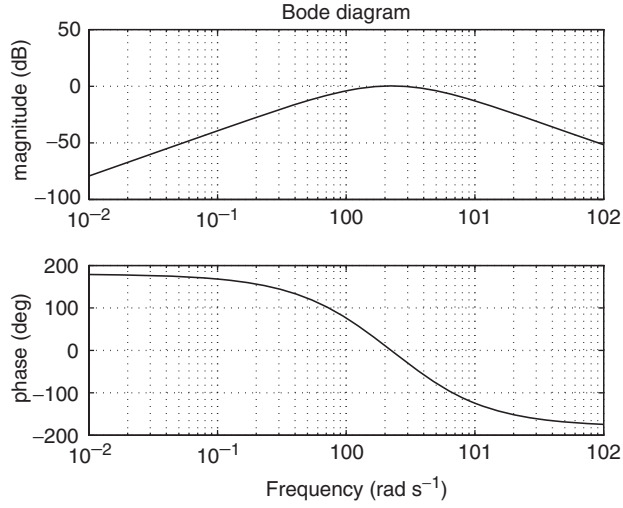

Figure 10. Bode plot of the open-loop system.

9. Conclusions

The key feature of the proposed method is that the underactuated system can be considered as a system

Downloaded By: [Aguilar, Luis T.] At: 20:24 28 April 2009

Table 1. Computed c_1 and c_2 values for several desired frequencies using DF method.

Desired Ω	Desired A_1	c_1	c_2	Experimental Ω	Experimental A_1
7	0.10	0.19	0.23	6.28	0.11
8	0.20	0.30	0.61	7.40	0.22
9	0.25	0.25	0.93	8.30	0.20
10	0.30	0.14	1.32	9.00	0.35

Table 2. Computed c_1 and c_2 values for several desired frequencies LPRS.

Desired Ω	Desired A_1	c_1	c_2	Experimental Ω	Experimental A_1
7	0.10	0.1856	0.2001	6.48	0.10
8	0.20	0.2589	0.5269	7.10	0.22
9	0.25	0.2450	0.9796	8.50	0.20
10	0.30	0.1134	1.65	9.20	0.35

Downloaded By: [Aguilar, Luis T.] At: 20:24 28 April 2009

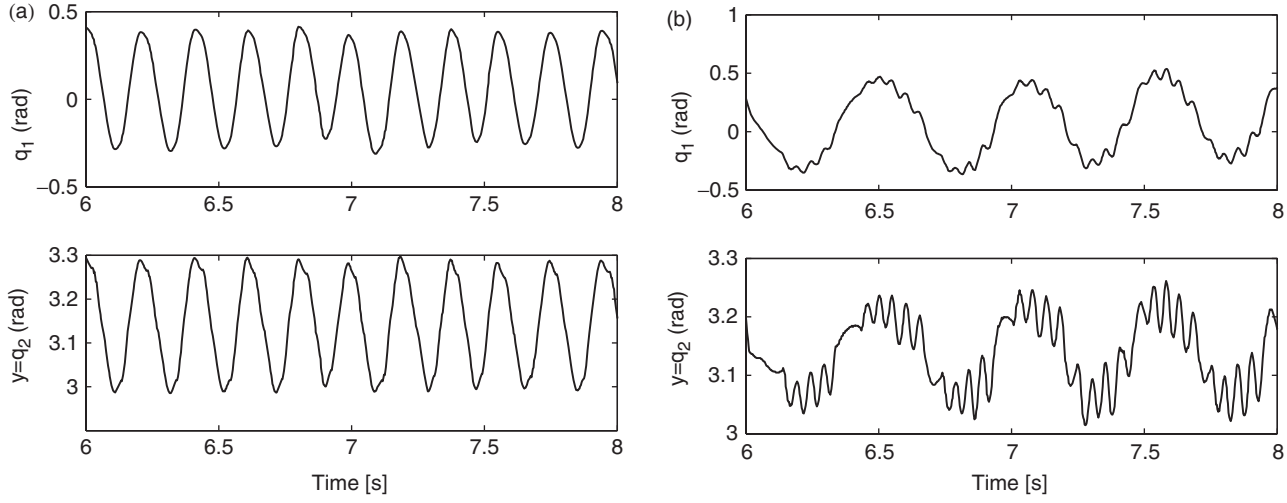

Figure 11. Steady state periodic motion of each joint where (a) is the periodic motion at $\Omega_1 = 25\,\mathrm{rad\,s^{-1}}$ and (b) is the periodic motion at $\Omega_2 = 10\,\mathrm{rad\,s^{-1}}$.

with unactuated dynamics with respect to actuated variables. For generation of self-excited oscillations with desired output amplitude and frequencies, a two-relay controller is proposed. The systematic approach for two-relay controller parameter adjustment is proposed. The DF method provides approximate values of controller parameters for the plants with the low-pass filter properties. The LPRS gives exact values of the controller parameters for the linear plants. The Poincaré maps provides the values of the controller parameters ensuring the existence of the locally orbitally stable periodic motions for an arbitrary mechanical plant. The effectiveness of the proposed design procedures is supported by experiments carried out on the Furuta pendulum from Quanser.

References

Aguilar, L., Boiko, I., Fridman, L., and Iriarte, R. (2009), 'Generating Self-excited Oscillations Via Two-relay Controller', *IEEE Transactions on Automatic Control*, 54(2), 330–335.

Atherton, D.P. (1975), *Nonlinear Control Engineering-Describing Function Analysis and Design*, Workingham, UK: Van Nostrand.

Boiko, I., Fridman, L., and Castellanos, M.I. (2004), 'Analysis of Second-order Sliding-mode Algorithms in the Frequency Domain', *IEEE Transactions on Automatic Control*, 49, 946–950.

Boiko, I. (2005), 'Oscillations and Transfer Properties of Relay Servo Systems – the Locus of a Perturbed Relay System Approach', *Automatica*, 41, 677–683.

Boiko, I., Fridman, L., Pisano, A., and Usai, E. (2007), 'Analysis of Chattering in Systems with Second-order

Sliding Modes', *IEEE Transactions on Automatic Control*, 52, 2085–2102.

Chevallereau, C., Abba, G., Aoustin, Y., Plestan, F., Canudas-de-Wit, C., and Grizzle, J.W. (2003), 'RABBIT: A Testbed for Advanced Control Theory', in *IEEE Control Systems Magazine*, 23, 57–79.

Craig, J. (1989), *Introduction to Robotics: Mechanics and Control*, Massachusetts, MA: Addison-Wesley Publishing.

Di Bernardo, M., Johansson, K.H., and Vasca, F. (2001), 'Self-oscillations and Sliding in Relay Feedback Systems: Symmetry and Bifurcations', *International Journal of Bifurcation and Chaos*, 11, 1121–1140.

Fantoni, I., and Lozano, R. (2001), *Nonlinear Control for Underactuated Mechanical Systems*, London: Springer.

Fridman, L. (2001), 'An Averaging Approach to Chattering', *IEEE Transactions on Automatic Control*, 46, 1260–1265.

Grizzle, J.W., Moog, C.H., and Chevallereau, C. (2005), 'Nonlinear Control of Mechanical Systems with an Unactuated Cyclic Variable', *IEEE Transactions on Automatic Control*, 50, 559–576.

Levant, A. (1993), 'Sliding Order and Sliding Accuracy in Sliding Mode Control', *International Journal of Control*, 58, 1247–1263.

Orlov, Y., Riachy, S., Floquet, T., and Richard, J.-P. (2006), 'Stabilization of the Cart-pendulum System via Quasi-homogeneous Switched Control', in *Proceedings of the 2006 International Workshop on Variable Structure Systems*, 5–7 June, 139–142.

Shiriaev, A.S., Freidovich, L.B., Robertsson, A., and Sandberg, A. (2007), 'Virtual-holonomic-constraints-based Design Stable Oscillations of Furuta Pendulum: Theory and Experiments', *IEEE Transactions on Robotics*, 23, 827–832.

Varigonda, S., and Georgiou, T.T. (2001), 'Dynamics of Relay Relaxation Oscillators', *IEEE Transactions on Automatic Control*, 46, 65–77.

Appendix A. Dynamic model of Furuta pendulum

The equation motion of Furuta pendulum, described by (1), was specified by applying the Euler–Lagrange formulation (Craig 1989), where

$$M(q) = \begin{bmatrix} M_{11}(q) & M_{12}(q) \\ M_{12}(q) & M_{22}(q) \end{bmatrix}, \quad H(q,\dot{q}) = \begin{bmatrix} H_1(q,\dot{q}) \\ H_2(q,\dot{q}) \end{bmatrix}$$

with

$$M_{11}(q) = J_{\text{eq}} + M_p r^2 \cos^2(q_1),$$

$$M_{12}(q) = -\frac{1}{2} M_p r l_p \cos(q_1)\cos(q_2),$$

$$M_{22}(q) = J_p + M_p l_p^2,$$

$$H_1(q,\dot{q}) = -2M_p r^2 \cos(q_1)\sin(q_1)\dot{q}_1^2 + \frac{1}{4} M_p r l_p \cos(q_1)\sin(q_2)\dot{q}_2^2$$

$$H_2(q,\dot{q}) = \frac{1}{2} M_p r l_p \sin(q_1)\cos(q_2)\dot{q}_1^2 + M_p g l_p \sin(q_2)$$

where $M_p = 0.027\,\text{Kg}$ is mass of the pendulum, $l_p = 0.153\,\text{m}$ is the length of pendulum centre of mass from pivot, $L_p = 0.191\,\text{m}$ is the total length of pendulum, $r = 0.0826\,\text{m}$ is the length of arm pivot to pendulum pivot, $g = 9.810\,\text{m}\,\text{s}^{-2}$ is the gravitational acceleration constant, $J_p = 1.23 \times 10^{-4}\,\text{Kg}\,\text{m}^{-2}$ is the pendulum moment of inertia about its pivot axis, and $J_{\text{eq}} = 1.10 \times 10^{-4}\,\text{Kg}\,\text{m}^{-2}$ is the equivalent moment of inertia about motor shaft pivot axis.

Downloaded By: [Aguilar, Luis T.] At: 20:24 28 April 2009